Mild Reductions in Mitochondrial Citrate Synthase Activity Result in a Compromised Nitrate Assimilation and Reduced Leaf Pigmentation But Have No Effect on Photosynthetic Performance or Growth[1][W]

Agata Sienkiewicz-Porzucek, Adriano Nunes-Nesi, Ronan Sulpice, Jan Lisec, Danilo C. Centeno, Petronia Carillo, Andrea Leisse, Ewa Urbanczyk-Wochniak, and Alisdair R. Fernie*

Max-Planck-Institut für Molekulare Pflanzenphysiologie, 14476 Golm, Germany (A.S.-P., A.N.-N., R.S., J.L., D.C.C., A.L., E.U.-W., A.R.F.); and Dipartimento di Scienze della Vita, Seconda Università degli Studi di Napoli, Via Vivaldi, 43 I–81100 Caserta, Italy (P.C.)

Transgenic tomato (*Solanum lycopersicum*) plants, expressing a fragment of the mitochondrial citrate synthase gene in the antisense orientation and exhibiting mild reductions in the total cellular activity of this enzyme, displayed essentially no visible phenotypic alteration from the wild type. A more detailed physiological characterization, however, revealed that although these plants were characterized by relatively few changes in photosynthetic parameters they displayed a decreased relative flux through the tricarboxylic acid cycle and an increased rate of respiration. Furthermore, biochemical analyses revealed that the transformants exhibited considerably altered metabolism, being characterized by slight decreases in the levels of organic acids of the tricarboxylic acid cycle, photosynthetic pigments, and in a single line in protein content but increases in the levels of nitrate, several amino acids, and starch. We additionally determined the maximal catalytic activities of a wide range of enzymes of primary metabolism, performed targeted quantitative PCR analysis on all three isoforms of citrate synthase, and conducted a broader transcript profiling using the TOM1 microarray. Results from these studies confirmed that if the lines were somewhat impaired in nitrate assimilation, they were not severely affected by this, suggesting the presence of strategies by which metabolism is reprogrammed to compensate for this deficiency. The results are discussed in the context of carbon-nitrogen interaction and interorganellar coordination of metabolism.

Citrate synthase catalyses the condensation reaction occurring between the four-carbon oxaloacetate molecule and the two-carbon acetyl-CoA molecule and is often regarded as the first committed step of the tricarboxylic acid cycle (TCA; Landschütze et al., 1995a, 1995b; Fernie et al., 2004). Despite the strategic positional importance of this enzyme, studies that have investigated its metabolic importance in plants remain at a premium (Scheible et al., 2000; Bläsing et al., 2005; Pracharoenwattana et al., 2005; Urbanczyk-Wochniak et al., 2006). That said, many focused studies have been directed on the role of this pathway in plant soil interactions. In this context, citrate synthase has been fiercely debated as an important determinant of root citrate exudation (Delhaize et al., 2001; Kochian et al., 2004), and as such as an important mediator of both phosphate uptake and aluminum tolerance (de la Fuente et al., 1997; Anoop et al., 2003). Moreover, a role for citrate synthase has been postulated in the process of floral development (Landschütze et al., 1995b; Yui et al., 2003). Although these studies have greatly enhanced our understanding of the role of citrate synthase in specific developmental and environmental interactions, they provide little information concerning the general role of isoforms of this enzyme in the regulation of plant respiration.

In recent years much research effort has been expended on elucidating the metabolic and physiological functions of the various isoforms of isocitrate dehydrogenase (Galvez et al., 1994; Hodges et al., 2003). In contrast, directed studies, such as those described above, but concerning the metabolic role of citrate synthase are rare (Pracharoenwattana et al., 2005) and do not directly concern the mitochondrial isoform. Despite this fact, studies at the pathway level have provided many interesting insights into the contribution of this isoform in, for example, the regulation of the nitrate assimilation pathway in the illuminated leaf. Such studies have predominantly been focused on the levels of the metabolic intermediates and mRNA levels of enzymes of the pathways in question (Scheible et al., 2000). However, the recent widespread adoption of genomic and postgenomic technologies has facilitated systematic analysis of the global response of metabolism to cellular circumstance (Bläsing et al., 2005; Urbanczyk-Wochniak et al., 2006; www.genevestigator.

[1] This work was supported in part by the Max-Planck-Gesellschaft (A.S.-P., A.N.-N., and A.R.F.) and in part by Coordenação de Aperfeiçoamento de Pessoal de Nível Superior (D.C.C.).

* Corresponding author; e-mail fernie@mpimp-golm.mpg.de.

The author responsible for distribution of materials integral to the findings presented in this article in accordance with the policy described in the Instructions for Authors (www.plantphysiol.org) is: Alisdair R. Fernie (fernie@mpimp-golm.mpg.de).

[W] The online version of this article contains Web-only data.
www.plantphysiol.org/cgi/doi/10.1104/pp.108.117978

ethz.ch), facilitating evaluation of cross-pathway, or even network responses, at both the transcript and metabolite level. As part of our own ongoing project to determine the function of the TCA cycle in the illuminated leaves, we have, thus far, characterized the *Aco*1 tomato (*Solanum pennellii*) mutant deficient in aconitase expression (Carrari et al., 2003), as well as transgenics of the cultivated tomato deficient in the expression of the mitochondrial isoforms of malate dehydrogenase (Nunes-Nesi et al., 2005), fumarase (Nunes-Nesi et al., 2007), and succinyl-CoA ligase (Studart-Guimarães et al., 2007). These genetic studies have generally corroborated those based on the use of mitochondrial inhibitors (for review, see Raghavendra and Padmasree, 2003; Sweetlove et al., 2007), in demonstrating a role for mitochondria in optimizing photosynthesis and are additionally in keeping with results from the analysis of plant genotypes directly affected in activities of proteins associated with normal functioning of the mitochondrial electron transport chain (see Sweetlove et al., [2007] for details). It is, however, worth noting that the characterization of manipulations of the TCA cycle revealed mixed results when addressed from the perspective of cellular metabolism in general. Intriguingly, manipulation of aconitase, fumarase, and the mitochondrial malate dehydrogenase appeared to have greater consequence than that of the mitochondrial reactions catalyzed by succinyl-CoA ligase and isocitrate dehydrogenase (Nunes-Nesi et al., 2005, 2007; Lemaitre et al., 2007; Studart-Guimarães et al., 2007). The former three manipulations displayed clear effects on the rate of both photosynthesis and respiration (Carrari et al., 2003; Nunes-Nesi et al., 2005, 2007), whereas the later two displayed no obvious physiological effects under optimized growth conditions (Lemaitre et al., 2007; Studart-Guimarães et al., 2007). In this study, we turn our attention to the evaluation of the importance of the mitochondrial citrate synthase—often described as the first committed step of the TCA cycle—for metabolism in the illuminated leaf. To continue our ongoing project to determine the function of the TCA cycle in the illuminated leaf we describe here the generation of transgenic plants exhibiting mild decreases in the expression of the mitochondrial isoform of citrate synthase. The transgenic lines generated were comprehensively characterized at biochemical, physiological, and transcriptional levels. Data accumulated in this study are discussed in terms of current models concerning the importance of the TCA cycle in the illuminated leaf as well as the coordination of plant carbon and nitrogen metabolism.

RESULTS

Cloning of a cDNA Encoding Mitochondrial Citrate Synthase from Tomato

Searching tomato EST collections (Van der Hoeven et al., 2003) revealed the presence of 17 ESTs encoding mitochondrial citrate synthase (mCS), all of which belonged to a single tentative consensus (TC180568) sequence. Assembly and sequence analysis of this gene revealed an open reading frame of 470 amino acids. Comparison with functionally characterized citrate synthases revealed 91% identity to potato (*Solanum tuberosum*; Q43175), 85% to Arabidopsis (*Arabidopsis thaliana*) CSY4 (At2g44350), 83% identity to Arabidopsis CSY5 (At3g60100), 56% identity to *Saccharomyces cerevisiae* Cit1p (NP_014398), 54% Cit2p (NP_009931), and 45% identity to *S. cerevisiae* Cit3p (NP_015325), which are all mitochondrial isoforms but a much lower identity (<30%) to peroxisomal isoforms (Fig. 1A). Moreover, the gene bears characteristics of a mitochondrial peptide sequence, indicating a mitochondrial location for the protein encoded. Analysis of mRNA northern blots using the *Sl*mCS cDNA as a probe indicates constitutive expression of the gene, with the transcript present at approximately equivalent levels in young and mature leaves, stems, and roots and ubiquitously during fruit development (data not shown).

Transgenic Plants Show Little Change in Growth Rate, Time of Flowering, or Fruit Set

A 1,195-bp fragment of the cDNA encoding mCS was cloned in antisense orientation between the cauliflower mosaic virus (CaMV) promoter and the *ocs* terminator (Fig. 1B). We then transferred 53 transgenic tomato plants obtained by *Agrobacterium tumefaciens*-mediated transformation to the greenhouse. A screening of the lines was performed by a combination of total cellular citrate synthase activity and northern-blot analyses (data not shown). These preliminary studies allowed the identification of nine lines that showed a considerably reduced mCS expression and a decrease in total CS activity. These lines were clonally propagated and transferred to the greenhouse. After a period of 6 weeks growth, leaves were harvested in the middle of the light period, and a secondary screen was carried out at the mRNA level (Fig. 1C). Following this screen we evaluated the absolute citrate synthase activities of four of these lines (Fig. 1D). When taken together these results demonstrate that these four lines (CS40, CS22, CS45, and CS25), were suitable for further study.

As a first experiment we grew the transgenic plants in the greenhouse side by side with wild-type controls. No clear difference could be observed in the growth of aerial parts of the plant (exemplified in Fig. 2A). Moreover, although the transgenics exhibited a trend toward decreased fruit yield, this was only significant in the case of line CS22 (data not shown). We next turned our attention to floral tissues because antisense inhibition of the potato homolog of *St*mCS has previously been characterized to confer a specific floral phenotype (Landschütze et al., 1995b). We were somewhat surprised to find little difference in the time of flowering in the transformants created here,

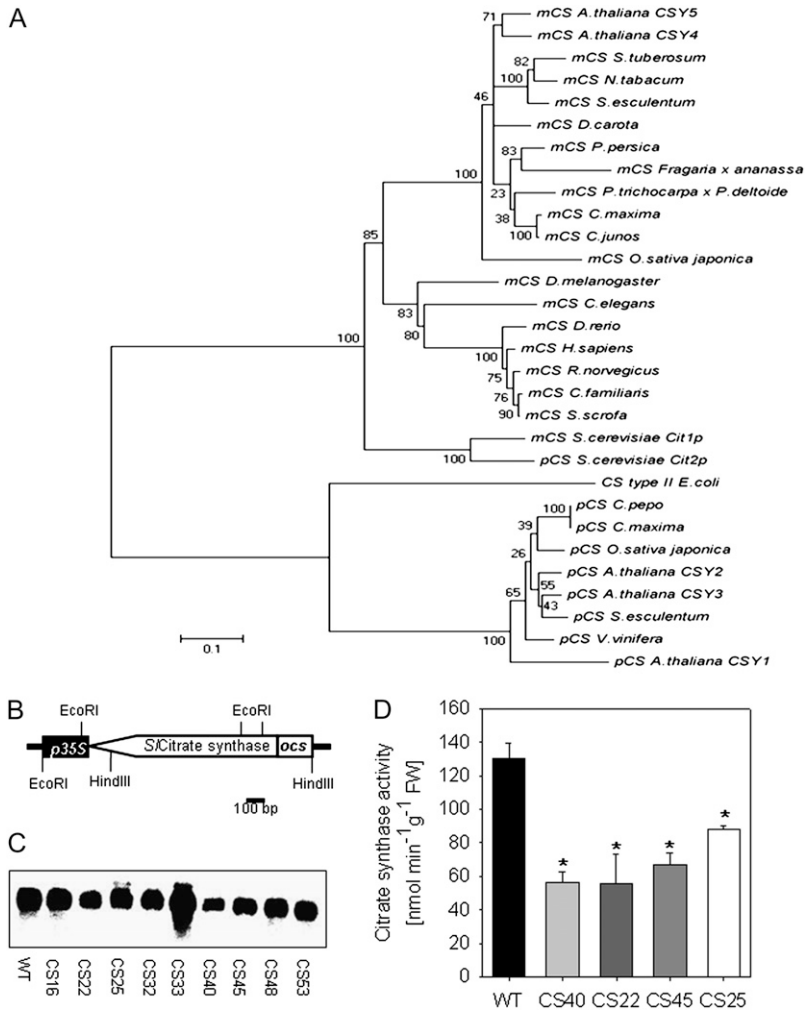

Figure 1. Characterization and expression of tomato mitochondrial citrate synthase. A, Dendogram of citrate synthase sequences. Citrate synthase sequences were aligned using the ClustalW alignment program (Higgins and Sharp, 1988). Neighbor-joining trees (Saitou and Nei, 1987) were constructed with MEGA4 software (Tamura et al., 2007). B, Construct of a chimeric gene for the expression of tomato mitochondrial citrate synthase antisense consisting of a 540-bp fragment encoding the CaMV 35S promoter and a 1,195-bp antisense fragment of the mitochondrial citrate synthase gene and the 200-bp *ocs* terminator. C, Northern-blot analysis of the expression of the mitochondrial citrate synthase gene of leaves of transgenic plants as compared to wild type. D, Total citrate synthase activity determined in 6-week-old leaves taken from fully expanded source leaves of transgenic plants with altered expression of citrate synthase as compared to the wild type. An asterisk indicates values that were determined by the *t* test to be significantly different ($P < 0.05$) from the wild type.

however, a slight, trend in the total number of flowers per plant was apparent (Fig. 2B). Given that several of our previous studies demonstrated that plants deficient in expression of the TCA cycle enzymes are characterized by altered rates of photosynthesis (see, for example, Nunes-Nesi et al. [2007]), we next evaluated this parameter in the transformants created here. Firstly, we studied the metabolism of $^{14}CO_2$ by leaf discs excised from the wild type and two of the transgenic lines. This study revealed no differences in the rate of carbon assimilation or in its subsequent metabolism into Suc, starch, organic, and amino acids (Fig. 2C). In a second approach we evaluated the assimilation rate by direct measurement of gas exchange under photon flux densities (PFD) that ranged from 100 to 1,000 μmol m^{-2} s^{-1} (Fig. 2D). Results from this study were complementary to those of the $^{14}CO_2$ feeding experiment in revealing no major difference in assimilation rate. However, when a third approach was taken, that of measuring the rate of chloroplastic electron transfer, this parameter was found to be significantly elevated in the transformants (Fig. 2E). Similarly, evaluation of gas exchange in the dark revealed that both lines CS40 and CS22 exhibited significantly elevated rates of respiration (Fig. 2F). Evaluation of the total protein and nitrogen content of the leaves of the transgenic lines revealed that these were largely unaltered. Although there was a significant decrease in the protein level in line CS45 (Fig. 2G), in no instance was the total nitrogen content altered.

Respiratory Parameters in the Transgenic Lines

Given the above indication of an altered respiration in darkened leaves we next studied respiratory fluxes in the illuminated leaf. For this purpose we adopted two strategies. First, we recorded the evolution of $^{14}CO_2$ following incubation of leaf discs in positionally labeled ^{14}C-Glc molecules, and secondly we performed gas chromatography-mass spectrometry (GC-MS) analysis on extracts from leaf discs following incubation in 20 mM ^{13}C-sodium pyruvate. In the first experiment, we incubated leaf discs taken from plants in the light and supplied these with [1-^{14}C], [2-^{14}C], [3,4-^{14}C], or [6-^{14}C]Glc over a period of 6 h. During this

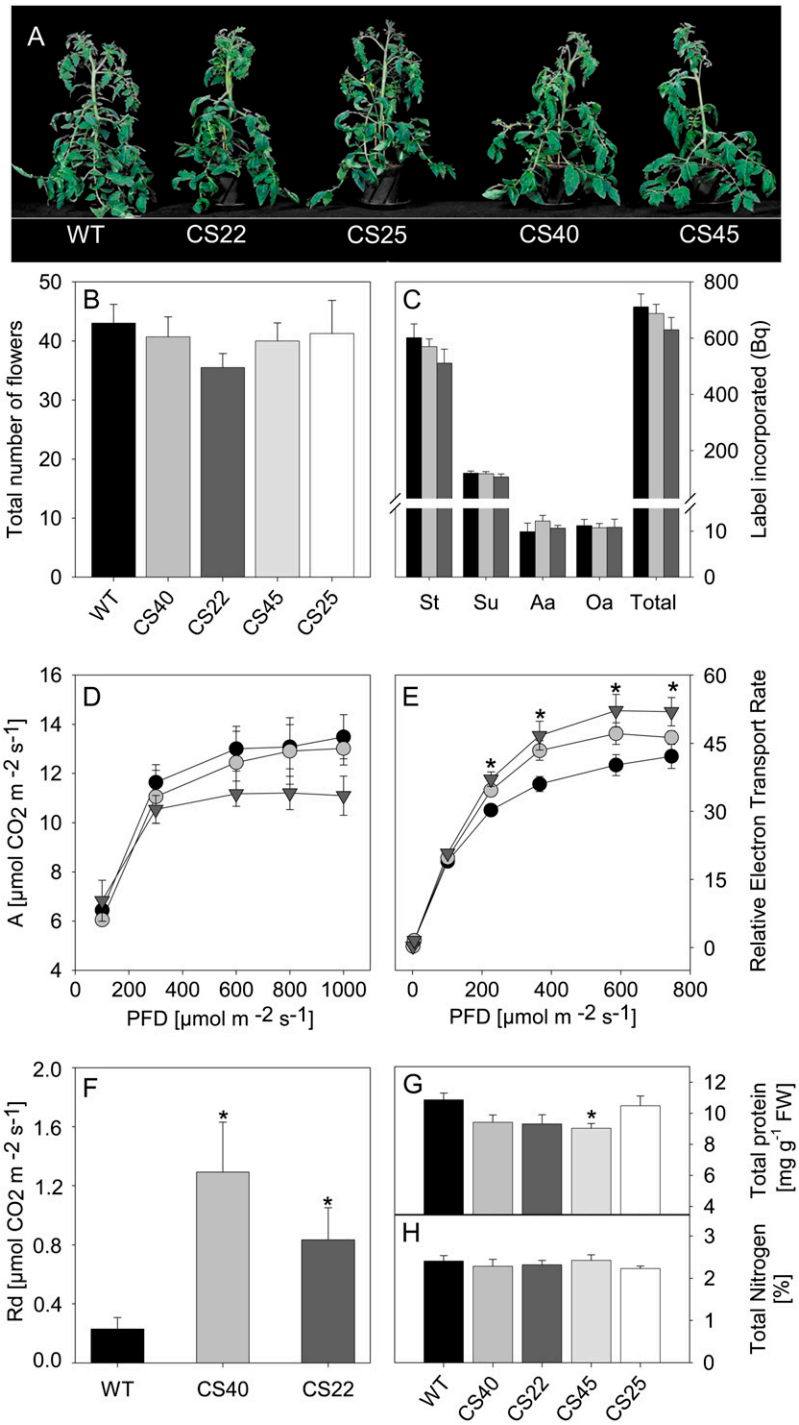

Figure 2. Physiological parameters of transgenic tomato plants displaying reduced activities of mitochondrial citrate synthase. A, Photograph showing representative plants after 5-week growth. B, Total number of flowers generated by transgenic and wild-type plants. C, Photosynthetic assimilation and partitioning at the onset of illumination. Leaf discs were cut from six separate untransformed tomato plants and two independent transgenic lines at the end of the night and illuminated at 250 μmol photosynthetically active radiation m^{-2} s^{-1} in an oxygen electrode chamber containing air saturated with $^{14}C0_2$. After 30 min the leaf discs were extracted and fractionated. St, Starch; Su, sugars; Aa, amino acids; Oa, organic acids; Total, total uptake. D, assimilation rate (A). E, In vivo chlorophyll fluorescence was measured as an indicator of the electron transport rate by use of a PAM fluorometer at PFDs ranging from 100 to 800 μmol m^{-2} s^{-1} . F, Dark respiration (Rd). G, Total protein. H, Total nitrogen content. Values are presented as mean ± SE of six individual determinations per line. All measurements were performed in 5- to 6-week-old plants. The lines used were: wild type, black circles and bars; CS40, dark grey triangles and grey bars; CS22, light grey circles and dark grey bars; An asterisk indicates values that were determined by the *t* test to be significantly different ($P < 0.05$) from the wild type.

time, we collected the $^{14}CO_2$ evolved at hourly intervals. Carbon dioxide can be released from the C_1 position by the action of the enzymes that are not associated with mitochondrial respiration, but carbon dioxide evolution from the $C_{3:4}$ positions of Glc cannot (ap Rees and Beevers, 1960). Thus, the ratio of carbon dioxide evolution from C_1 to $C_{3:4}$ provides an indication of the relative rate of the TCA cycle with respect to the other processes of carbohydrate oxidation. When the relative rate of $^{14}CO_2$ evolution of the transgenic and wild-type lines is compared for the various substrates an interesting picture emerges (Fig. 3A). Although the rate of $^{14}CO_2$ evolution is generally higher in leaves incubated in [1-^{14}C]Glc, it is interesting to note that there is a tendency of increased absolute evolution from the C_1 position in the transgenic lines and an even greater (and significant) increase in the evolution from the C_2 position. There was also a marked increase

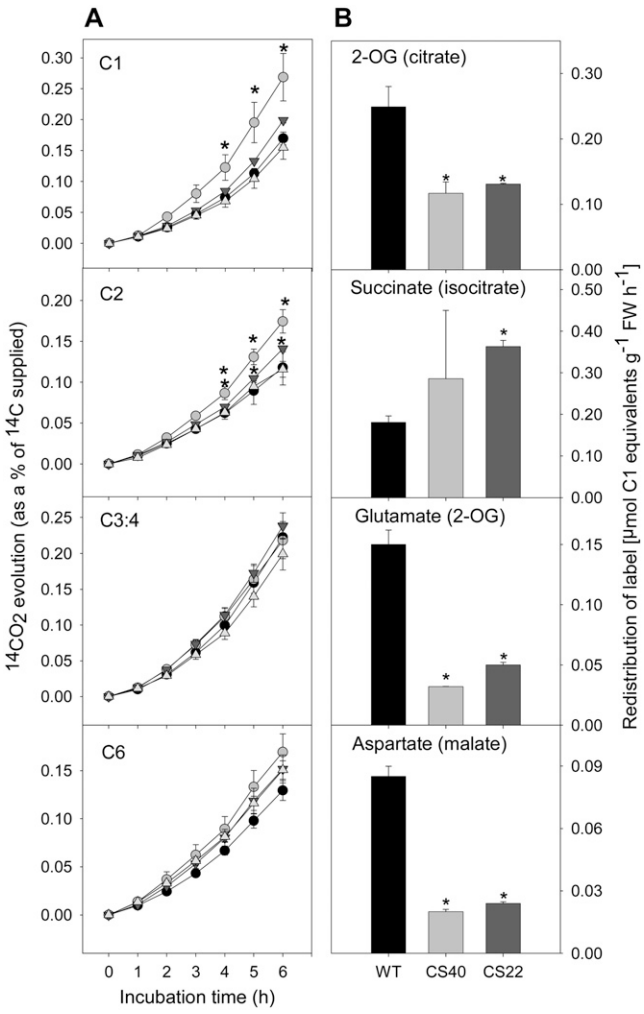

Figure 3. Respiratory parameters in leaves of the antisense mitochondrial citrate synthase lines. A, Evolution of $^{14}CO_2$ from isolated leaf discs in the light. The leaf discs were taken from 5-week-old plants and were incubated in 10 mM MES-KOH solution, pH 6.5, 0.3 mM Glc supplemented with 2.32 kBq mL^{-1} of [1-^{14}C]-, [2-^{14}C]-, [3,4-^{14}C]-, or [6-^{14}C]Glc at an irradiance of 200 μmol m^{-2} s^{-1}. The $^{14}CO_2$ liberated was captured (at hourly intervals) in a KOH trap and the amount of radiolabel released was subsequently quantified by liquid scintillation counting. B, Redistribution of label following feeding of isolated leaves in [U-^{13}C]pyruvate via the petiole (see "Materials and Methods") in CS transgenics and wild-type plants. The substrate is indicated within brackets, following the name of the product. The lines used were: wild type, black circles; CS22, light grey circles; CS40, dark grey triangles; CS45, light grey triangles. Asterisks indicate values that were determined by the *t* test to be significantly different ($P < 0.05$) from the wild type.

in the $C_1/C_{3:4}$ ratio of line CS22 indicating a decrease in the relative rate of TCA cycle oxidation in this line. To further investigate this we performed analyses of isotope distribution in the wild type and lines CS22 and CS40. For this purpose leaves were incubated in medium containing ^{13}C-labeled pyruvate for a period of 3 h and the redistribution of heavy label was followed using an established GC-MS protocol. These studies indicate that the rate of isotope redistribution between citrate and 2-oxoglutarate was markedly reduced in the transgenic as was that between 2-oxoglutarate and Glu and between malate and Asp (Fig. 3B). In contrast, the rate of redistribution between isocitrate and succinate was unaltered or even (in the case of line CS22) increased. Taken together these data and that from the respiration measurements described above, hint toward a restriction in pyruvate-derived fluxes through citrate synthase and nitrate assimilation, but suggest that succinate supply to the mitochondrial electron transport chain is enhanced, rather than diminished in the transformants.

Changes in Primary Carbon Metabolism in the Transformants

Analysis of the carbohydrate content of leaves from 6-week-old plants during a diurnal cycle revealed that the transformants were characterized by increases in the levels of Glc, Fru, Suc, and starch; however, due to the previously reported high variance in the levels of these metabolites in this species (Studart-Guimarães et al., 2007), these increases were not significant (data not shown). We next extended these studies, to encompass other major pathways of primary metabolism, by utilizing an established GC-MS protocol for metabolic profiling that facilitates the quantification of some 70 metabolites (Fernie et al., 2004). The full data set (Fig. 4, A and B; Supplemental Fig. S1) revealed considerable differences between the transgenics and the wild type with several increases in the contents of a range of sugars and non-TCA cycle organic acids (Supplemental Fig. S1). In contrast, as would perhaps be expected, the lines generally contained elevated levels of TCA cycle intermediates with significant decreases observed in citrate (lines CS40 and CS22), citramalate (all lines), and malate (line CS22; Fig. 4A). That said, line CS40 displayed elevated levels of succinate, whereas both lines CS40 and CS22 were characterized as containing significantly elevated levels of 2-oxoglutarate. Evaluation of nucleotides in a subset of the transgenic lines revealed that these were largely unaltered in the transgenics with the exception that the levels of UDP-Glc were decreased (data not shown). In contrast, large changes were observed in the amino acid profile of the transformants (Fig. 4B). Decreases were observed in the levels of Ala, Asp, and γ-aminobutyrate in at least two of the transformants, whereas Tyr, Trp, Phe, Gly, Gln, and Asn increased, up to 8-fold in at least two of the transformants. The branched chain amino acids Val and Ile were largely unaltered in these lines (Supplemental Fig. S1).

Evaluation of Diurnal Changes in Amino Acid Levels

Given that there is considerable diurnal variation in the levels of amino acids, we next evaluated whether this was altered in the transgenics. For this purpose we collected samples at five different time points during a

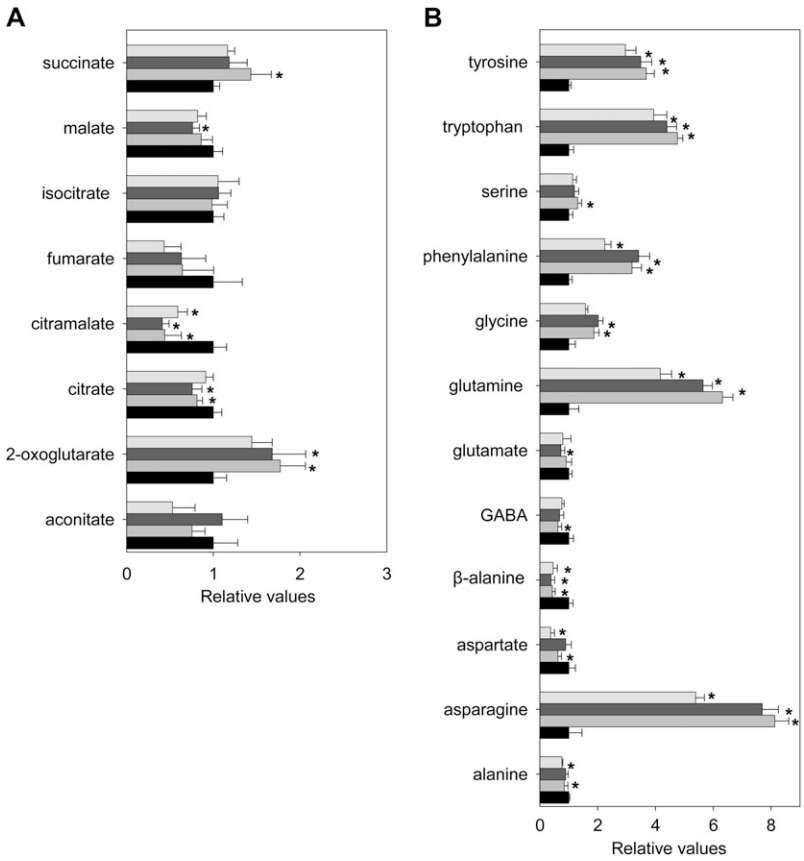

Figure 4. Relative metabolite content of fully expanded leaves from 6-week old plants of the antisense mitochondrial citrate synthase lines. Metabolites were determined as described in ''Materials and Methods''. Data are normalized with respect to the mean response calculated for the wild type (to allow statistical assessment, individual samples from this set of plants were normalized in the same way). Values are presented as mean ± SE of determinations on six individual plants per line. Asterisks indicate values that were determined by the *t* test to be significantly different ($P < 0.05$) from the wild type. The lines used were: wild type, black bars; CS40, grey bars; CS22, dark grey bars; CS45, light grey bars.

24-h cycle and determined the amino acid levels by HPLC. Using this method allowed us to evaluate the behavior of nine of the amino acids in the wild type and in lines CS40 and CS22 (Fig. 5). The samples taken in the middle of the day (12 h) are generally in good accordance with those presented in Figure 4—with large increases in the levels of Gln and Asn. However, the decrease in Ala mentioned above was only visible in a single line in this second experiment. Interestingly, when the dynamics of these metabolites over time is considered, the differences in the levels of Gln and Asn in the transgenic lines are at their maximum at the end of the day/beginning of the night after which they return to more or less wild-type levels. These data also support the observation based on our GC-MS data that the branched chain amino acids were largely unaltered and Ser was elevated in the transformants.

Effect of Reduction of Mitochondrial Citrate Synthase on the Activities of Other Enzymes of Primary Metabolism

Because some of the changes in metabolites described above were contrary to what had been expected, we next analyzed the maximal catalytic activities of a wide range of important enzymes of photosynthetic carbon metabolism (Table I). The transgenic lines were characterized by changes in a wide range of these enzymes displaying clear decreases in AGPase (in three of the four transgenics), cytosolic Fru-1,6-bisphosphatase, Gln synthetase, the NADP-dependent isoform of isocitrate dehydrogenase, and nitrate reductase (in all lines), and both initial and total activities of NADP-dependent malate dehydrogenase (in the most strongly inhibited lines—CS22 and CS40). In contrast, the levels of acid invertase increased in line CS45, however, changes in these activities were not consistent with the change in citrate synthase activity indicating that they were most likely a pleiotropic effect. Activities of fructokinase, hexokinase, Glc-6-P dehydrogenase, NAD-isocitrate dehydrogenase, ATP-dependent phosphofructokinase, and succinyl-CoA ligase were invariant across the lines (Supplemental Table S1).

Nitrate Content in the Transgenic Lines

Given that some of the changes in amino acid metabolism reported above were somewhat unexpected we thought it prudent to directly check the leaf nitrate content. For this reason we spectrophotometrically assayed this. These assays revealed that the transgenics reproducibly contained up to 5- to 6-fold increases in the content of the ion (2.34 ± 0.35, 11.80 ± 3.87, 14.37 ± 4.01, 4.54 ± 1.24, and 4.68 ± 1.48 μmol g^{-1} fresh weight for wild type, CS22, CS40, CS25, and CS45, respectively), and are in keeping with the observed reduction in the activities of enzymes associated with nitrate assimilation documented above.

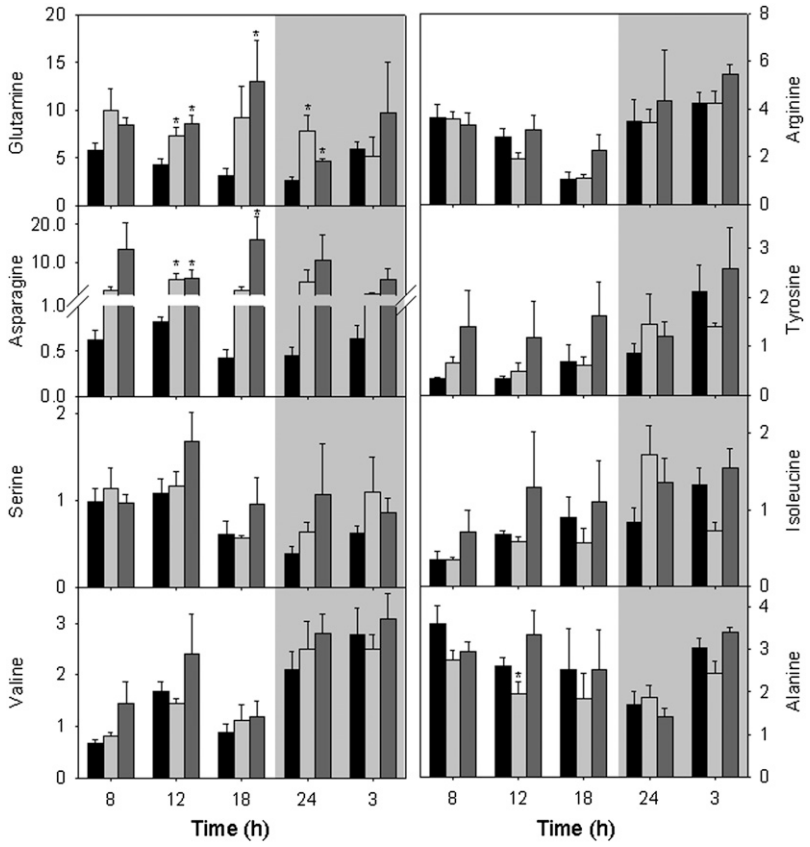

Figure 5. Diurnal changes in leaf amino acids content in leaves of 6-week-old plants of the antisense mitochondrial citrate synthase lines. At each time point, samples were taken from mature source leaves, and the data are presented as μmol g^{-1} fresh weight and represent the mean $\pm$ SE of measurements from three plants per genotype. An asterisk indicates values that were determined by the *t* test to be significantly different ($P < 0.05$) from the wild type. Grey bars, dark period; white bars, light period. The lines used were: wild type, black bars; CS40, grey bars; CS22, dark grey bars.

Furthermore, when considered alongside the total leaf nitrogen content, these data reveal that the lines are not deficient in the transport of nitrate but merely in its utilization.

Pigment Contents in the Transgenic Lines

Given the above results we next decided to evaluate the levels of the photosynthetic pigments because these compounds have often been reported as important indicators of nitrogen deficiencies (Gaude et al., 2007). HPLC analysis revealed that chlorophyll *a* and *b* were both significantly reduced in the transformants as were β-carotene, violaxanthin, and neoxanthin (in all cases these changes were significant in at least three of the transgenic lines; Fig. 6). The decrease in the contents of the photoprotective xantophyll cycle intermediates is likely to diminish their function (Bassi et al., 1997), however, given that the plants were not under conditions of light stress, it cannot explain the unexpectedly high chloroplastic electron flow observed in our fluorescence experiments described above.

Expression Levels of Other Isoforms of Citrate Synthase and Other Genes

To understand the failure to detect a decreased rate of respiration in the transformants, we next evaluated the expression of isoforms of citrate synthase using an established quantitative reverse transcription (RT)-PCR protocol (Czechowski et al., 2004). This revealed that while one of the peroxisomal isoforms was invariant across the genotypes the other was markedly increased (Fig. 7), suggesting that this isoform could partially compensate for changes in the expression of the mitochondrial isoform. To gain a broader overview of such compensatory processes we additionally evaluated the level of a wide range of transcripts using the commercially available TOM1 microarray. This revealed that the transformants were not characterized by massive global changes in gene expression. However, a few interesting trends emerged from these analyses. As would be expected, these microarrays reinforced the notion that one of the peroxisomal citrate synthases was up-regulated but also revealed a range of other minor changes (the full data set can be viewed in Map-Man format (Usadel et al., 2005) in Supplemental Figure S2. At the process level, statistical changes (see Usadel et al. [2006] for details), are apparent in light and dark reactions of photosynthesis, Suc and starch metabolism, photorespiration, mitochondrial electron transport, and metal handling as well as in redox regulation, flavonoid synthesis, and protein degradation. Moreover, decreased transcript levels were observed for transcripts associated with catalases, cell wall degrading enzymes, and tetrapyrole synthesis.

Table I. *Enzyme activities in antisense mitochondrial citrate synthase lines*

Activities were determined in 6-week-old fully expanded source leaves harvested 6 h into the photoperiod. Data presented are mean ± SE of measurements from six independent plants per genotype; values set in bold type were determined by the *t* test to be significantly different ($P < 0.05$) from the wild type.

	Wild Type	CS40	CS22	CS25	CS45
Enzymes			*nmol min^{-1} g^{-1} FW*		
AGPase	1211.73 ± 22.06	1217.43 ± 96.19	**902.73 ± 78.71**	**890.54 ± 130.04**	**923.49 ± 122.81**
Fru-1,6-bisphosphatase (cytosolic)	140.34 ± 16.73	**95.05 ± 14.00**	**89.81 ± 17.35**	**55.35 ± 4.41**	**51.91 ± 5.28**
Gln synthetase	1868.23 ± 312.56	**967.12 ± 238.28**	**611.12 ± 227.54**	**356.57 ± 129.11**	**257.81 ± 61.84**
NADP-isocitrate dehydrogenase	1032.39 ± 110.07	**674.01 ± 45.48**	**600.4 ± 99.24**	**690.08 ± 99.32**	**711.17 ± 86.66**
Malate dehydrogenase initial (NADP)	51.31 ± 3.23	40.64 ± 3.59	**33.31 ± 5.40**	**47.6 ± 7.26**	54.03 ± 3.56
Malate dehydrogenase total (NADP)	110.28 ± 8.79	89.08 ± 5.74	**78.23 ± 5.58**	**113.83 ± 5.89**	113.05 ± 7.48
Nitrate reductase	389.48 ± 33.13	**206.07 ± 26.42**	**237.57 ± 47.01**	**50.17 ± 35.25**	**155.27 ± 49.55**
PEP carboxylase	745.56 ± 38.31	**618.41 ± 31.83**	**528.13 ± 30.99**	**620.49 ± 20.32**	**621.88 ± 28.12**
Phosphoglucomutase	7208.23 ± 314.61	**4990.02 ± 267.94**	**4570.91 ± 321.14**	**6375.39 ± 342.31**	**6082.76 ± 399.16**
Shikimate dehydrogenase	582.86 ± 49.34	**471.48 ± 44.28**	**403.21 ± 32.41**	**415.18 ± 35.33**	**426.8 ± 27.17**

There are, however, at least some inconsistencies when the microarray results are compared at the single gene level to the changes in enzyme activities reported above. While, as would perhaps be expected, the transcript levels of the high-affinity nitrate transporter and of several genes encoding enzymes of glycolysis decreased, surprisingly the expression of Glu synthetase and the NADH-dependent Glu dehydrogenase were over 2-fold increased. That said the NADH-dependent GOGAT was abundant at significantly lower transcript levels in the transformant. Moreover, it is important to note that the TOM1 array offers far less than full-genome coverage and thus other important isoforms of any enzyme in question could be absent from the chip. Analysis of transcripts associated with regulation revealed two further interesting changes, namely altered expression of the bHLH and Dof finger transcription factor families, both of which have previously been characterized in the regulation of nitrogen assimilation (Yanagisawa, 2004; Lea et al., 2007). However, caution is needed in interpreting these findings given recent studies indicating the lack of a linear relationship between transcript response and cellular protein levels (Gibon et al., 2004).

DISCUSSION

Much recent research into plant photosynthetic energy metabolism has revealed an important functional role for respiratory metabolism in the illuminated leaf. The results of biochemical (Raghavendra and Padmasree, 2003), light environmental (Igamberdiev et al., 2001), and genetic (Bartoli et al., 2005; Sweetlove et al., 2006) manipulation of components of the mitochondrial electron transport chain indicate that its correct functioning is required to sustain optimal rates of photosynthesis. More recently both forward and reverse genetic strategies have revealed that manipulation in several activities of the TCA cycle also display a clear photosynthetic phenotype with deficiencies in aconitase or the mitochondrial malate dehydrogenase resulting in elevated rates of photosynthesis (Carrari et al., 2003; Nunes-Nesi et al., 2005) whereas that in fumarase resulted in a severe repression of photosynthesis (Nunes-Nesi et al., 2007). In contrast, the anti-

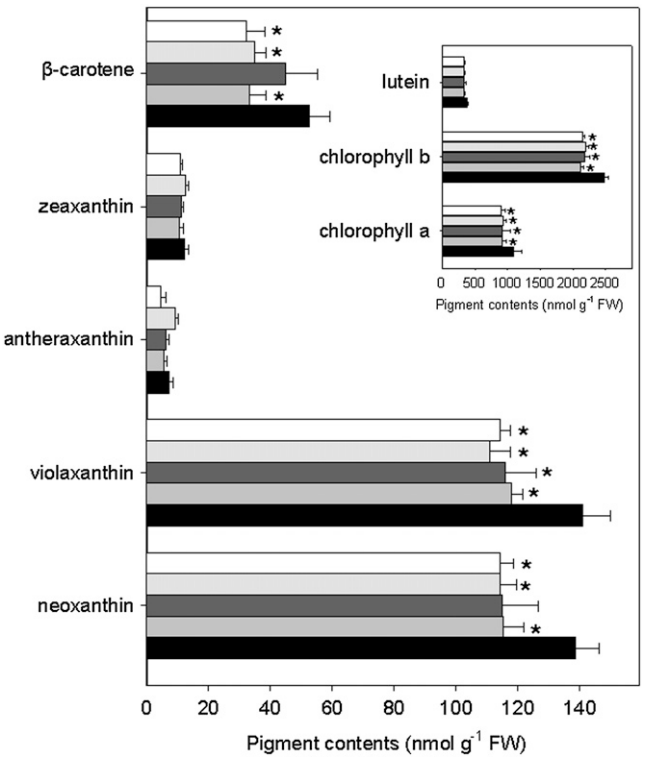

Figure 6. Pigment content of antisense mitochondrial citrate synthase lines. Pigments were determined in 6-week-old fully expanded source leaves. Samples used were harvested at exactly the same time as those for enzyme determinations presented in Table I. Values presented are mean ± SE of six individual plants per line. Asterisks indicate values that were determined by the *t* test to be significantly different ($P < 0.05$) from the wild type. The lines used were: wild type, black bars; CS40, grey bars; CS22, dark grey bars; CS45, light grey bars; CS25, white bars.

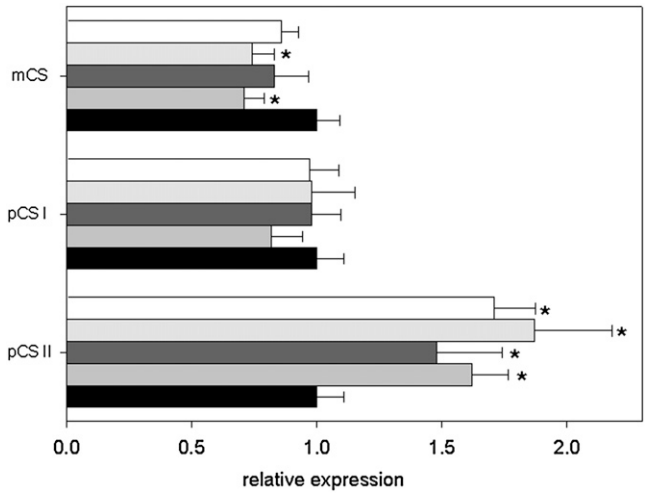

Figure 7. Relative transcript abundance of the various cellular isoforms of citrate synthase. The abundance of citrate synthase mRNAs was measured by semiquantitative RT-PCR. Values are presented as mean ± SE of determination on six individual plants per line. An asterisk indicates significantly different ($P < 0.05$) values obtained for each line in comparison to wild type as determined by the *t* test. mCS, Mitochondrial isoform; pCS I and II, peroxisomal isoforms (TC162670 and TC165584, respectively). The lines used were: wild type, black bars; CS40, grey bars; CS22, dark grey bars; CS45, light grey bars; CS25, white bars.

sense citrate synthase plants described here displayed largely unaltered rates of photosynthesis, despite showing clear alterations in metabolism, suggesting that the cell can compensate the decreased mitochondrial citrate synthase expression in the transformants. In light of this fact it is quite surprising that we were only able to recover plants with such mild reductions in activity (particularly when it is considered that Landschütze et al. [1995b] were able to produce transgenic potato with a mere 6% rest activity). Although it is possible that the peroxisomal citrate synthase provides a higher contribution to the total activity in the tomato than the potato, this seems unlikely to account for such a large discrepancy in the degree of inhibition. We also cannot exclude a threshold level of citrate synthase below which tomato could not regenerate, however, we think this improbable. A further possibility would be that there is a second, as yet unidentified, mitochondrial isoform of citrate synthase in tomato. However, the extreme similarity of the tomato and potato genomes does not support this hypothesis. Given these arguments, the hypothesis we favor is that the difference is most likely due to the relative effectiveness of the antisense inhibition itself. The results presented here also suggest an up-regulation of peroxisomal citrate synthase so it is possible that this up-regulation masks some of the down-regulation of the mitochondrial isoform. This up-regulated expression is able to compensate, at least in part, for the deficiency of mitochondrial citrate synthase. In such a scenario, citrate produced during operation of the glyoxylate cycle could either be further metabolism within the peroxisome or exported and subsequently taken up into the mitochondria, either in the form of citrate or isocitrate, in counterexchange for oxaloacetate via the operation of a previously characterized carboxylic acid transporter (Picault et al., 2002). It is possible that the oxaloacetate exported from the mitochondria could subsequently be taken up by the peroxisome to maintain the activity of the peroxisomal citrate synthase. However, whether this occurs in vivo, or if it is rather first converted to Asp before import, remains contentious (Mettler and Beevers, 1980; Pracharoenwattana et al., 2005). Regardless of the exact substrate imported into the peroxisome there is considerable evidence for strong coordination of metabolism between peroxisomal and mitochondrial processes that extends beyond their combined operation in pathways, such as photorespiration, which are shared between multiple organelles. The results we present here concerning plants deficient in mitochondrial citrate synthase are consistent with those of other laboratories in demonstrating a clear role for the peroxisomal production of citrate, in conjuncture with the operation of the mitochondrial TCA cycle, in respiration of acetyl units from peroxisomal β-oxidation of fatty acids (Raymond et al., 1992; Hooks, 2002; Pracharoenwattana et al., 2005). They also help to explain previous observations that peroxisomal citrate synthase activity is detected in a wide range of tissues and not only those in which the glyoxylate cycle is active (Cornah and Smith, 2002; Pracharoenwattana et al., 2005).

Although the restriction in mitochondrial citrate synthase activity had no major consequences on growth or plant physiology, it did result in considerable shifts in metabolism. Most dramatic among these was the concerted down-regulation of enzymes of nitrate assimilation. Analysis of mRNA levels by microarray revealed that several transcripts associated with nitrogen metabolism were repressed; however, this trend was not universal suggesting that the reduction in nitrate assimilation was, at least in part, mediated at the posttranslational level. Evaluation of steady-state metabolite levels were, by and large, in keeping with a restriction in nitrate assimilation. First, the level of nitrate was elevated in the transgenic lines, although it should be noted that the total leaf nitrogen content was unaltered in the transgenics. Secondly, the levels of several amino acids were reduced in the transformants. Thirdly, the increased levels of starch and soluble carbohydrates and the decreased levels of photosynthetic pigments observed in the transformants are diagnostic of a reduced rate of nitrate assimilation (Fritz et al., 2006; Gaude et al., 2007). That said, despite the clear restriction in nitrate assimilation, the levels of both Asn and Gln were significantly increased in the transformants described here. The increase of these metabolites under nitrate limitation is not without precedence since Orsel et al. (2006) recently reported a similar observation in Arabidopsis. Analysis of changes in the diurnal levels of Asn and

Gln revealed that they were less different at the end of the dark period—a fact that supports our hypothesis that these differences are somehow related to the changes in nitrate assimilation seen in these lines. Furthermore our data, when taken together, would seem to suggest that this increase may be due, at least in part, to an increased protein degradation and differential amino acid mobilization within the transformants. For instance, there is a clear up-regulation of genes associated with protein degradation in the transformants (see Supplemental Fig. S2) and in the rate of metabolism of the high-nitrogen amino acids (data not shown), suggesting that the lines may well exhibit altered rates of protein turnover. Contrary to this argument is the fact that the steady-state protein levels did not greatly vary in the lines. The changes in metabolism observed in these lines are highly interesting because they show an accumulation of soluble compounds with high-energy storage capacity suggesting that the cell adjusts for the lack of mitochondrial citrate synthase activity by accumulating slightly less long-term energy stores such as protein and chlorophyll. Indeed, many aspects of the metabolite profiles of the mitochondrial citrate synthase plants, including the accumulation of Gln and Asn, are reminiscent of those reported during extended night treatment or even during dark-induced senescence (Ishizaki et al., 2005; Gibon et al., 2006; Fahnenstich et al., 2007).

The recorded reduction in flux through mitochondrial steps of the TCA cycle could also be anticipated to lead to a reduced mitochondrial ATP and NAD(P)H production. Although we did not measure the latter and the steady-state levels of the former were unaltered, this postulate may additionally explain the severe apparent decrease in the in vivo activity of nitrate reductase since both ADP and NAD have been reported to inhibit the activity of this enzyme in vitro (Campbell and Smarrelli, 1978; Maldonado et al., 1978). Furthermore, the fact that the nitrate accumulation was so pronounced whereas the reduction in nitrate reductase activity seen here was relatively mild suggests that it is likely that such posttranslational regulation is taking place here. In addition the data described here provide several insights concerning both the coordination of respiration in the illuminated leaf and the importance of the mitochondrial citrate synthase in the mediation of carbon-nitrogen interactions. Although it is clear that the relatively mild decrease in mitochondrial citrate synthase activity has dramatic consequences on both the rate of nitrate assimilation and the rate of flux through the TCA cycle, the effects of this repression cannot be seen in the steady-state levels of the high-nitrogen amino acids Asn and Gln, suggesting that the cell can adjust to such a perturbation via the up-regulation of other pathways. The fact that the peroxisomal citrate synthase can apparently compensate for deficiency in the expression of the mitochondrial isoform is highly interesting especially given the fact that the reduction imposed was relatively mild. Because the up to 40% reduction in expression is well within ranges reported in the literature under a variety of conditions (see, for example, http://www.genevestigator.ethz.ch), it would appear likely that this finding is of physiological relevance. Interestingly, in this respect, is the reduced level of photosynthetic pigments in the transformants, which we believe to be a part of the general reprogramming of metabolism following the inhibition of nitrate assimilation. However, in this study we were unable to identify the exact mechanism underlying the reduction in the levels of these pigments. It can, however, be anticipated that further developments of methods to determine metabolite levels at subcellular resolution (Farre et al., 2001) and their eventual coupling to GC-MS-based flux profiling methods (Baxter et al., 2007) will allow a more detailed dissection of their metabolic regulation in the future.

MATERIALS AND METHODS

Materials

Tomato (*Solanum lycopersicum*) 'Moneymaker' was obtained from Meyer Beck. Plants were handled as described in the literature (Carrari et al., 2003). All chemicals and enzymes used in this study were obtained from Roche Diagnostics with the exception of radiolabeled sodium bicarbonate and D-(1-^{14}C) and D-(6-^{14}C) glucoses, which were from Amersham International, D-(2-^{14}C) and D-(3,4-^{14}C) glucoses were from American Radiolabeled Chemicals, and ^{13}C pyruvate was from Cambridge Isotope Laboratories.

cDNA Cloning and Expression

The 1,195-bp fragment of the mitochondrial citrate synthase enzyme was cloned in antisense orientation into the vector pBINAR (Liu et al., 1999) between the CaMV 35S promoter and the *ocs* terminator. This construct was introduced into plants by an *Agrobacterium*-mediated transformation protocol, and plants were selected and maintained as described in the literature (Tauberger et al., 2000). Initial screening of 53 lines was carried out using a combination of activity and mRNA measurements. These screens allowed the selection of four lines, which were chosen for subsequent physiological characterization.

RNA Extraction and Quantification

Total RNA was isolated using the commercially available Trizol kit (Gibco BRL) according to the manufacturer's suggestions for the extraction from plant material. Hybridization using standard conditions was carried out using the ESTs for the cytosolic isoform of citrate synthase obtained from the Clemson State University collection. Due to their relatively low expression, the transcript levels of all other isoforms of citrate synthase were determined by an established quantitative PCR method (Czechowski et al., 2004), using primers based on the ESTs of the Clemson State University collection. Microarray analysis was carried out exactly as described in Urbanczyk-Wochniak et al. (2006).

Analysis of Enzyme Activities

Enzyme extracts were prepared as described previously (Gibon et al., 2004), except that Triton-X 100 was used at a concentration of 1% and glycerol at 20%. Citrate synthase, isocitrate dehydrogenase (NAD), and phosphofructokinase (ATP) were assayed as described in Nunes-Nesi et al. (2007). Succinyl-CoA ligase was assayed as described in Studart-Guimarães et al. (2007). Malate dehydrogenase (NADP) was assayed as described in Scheibe and Stitt (1988). AGPase, phosphofructokinase (PPi), Suc-P synthase, cytosolic Fru-1,6-bisphosphatase, glucokinase, fructokinase, Glc-6-P dehydroge-

nase, NADP-isocitrate dehydrogenase, shikimate dehydrogenase, PEP carboxylase, acid invertase, ferredoxin-dependent GOGAT, nitrate reductase, and Gln synthetase were assayed as described in Gibon et al. (2004). Cytosolic and plastidial phosphoglucose isomerase were assayed as described in Weeden and Gottlieb (1982). Phosphoglucomutase was assayed as described in Manjunath et al. (1998).

Determination of Metabolite Levels

Leaf samples were taken at the time point indicated, immediately frozen in liquid nitrogen, and stored at −80°C until further analysis. Extraction was performed by rapid grinding of tissue in liquid nitrogen and immediate addition of the appropriate extraction buffer. The levels of starch, Suc, Fru, and Glc in the leaf tissue were determined exactly as described previously (Fernie et al., 2001). Pigments were determined as described in Bender-Machado et al. (2004). The levels of all other metabolites were quantified by GC-MS exactly following the protocol described by Roessner et al. (2001) with the exception that peak identification was optimized to tomato tissues (Roessner-Tunali et al., 2003) and extended to include newly identified peaks (Kopka et al., 2005; Schauer et al., 2005).

Nitrate and Nitrogen Determinations

Nitrogen content was determined in lyophilized, oven-dried fine-powdered leaves by combustion in an Elemental Analyzer EA1110 (Carlo Erba Strumentazioni); 5-mg samples were preweighed in tin containers together with 20 mg of tungstic anhydride prior to dropping into the reactor, which was maintained at 900°C with an excess of oxygen, to allow combustion. The oxides produced were separated by gas chromatography and quantified by a thermal conductivity detector by reference to standard compounds with known elemental composition (Friis et al., 1998). Nitrate was determined as detailed in Fritz et al. (2006).

Measurements of Photosynthetic Parameters

The ^{14}C-labeling pattern of Suc, starch, and other cellular constituents was performed by illuminating leaf discs (10-mm diameter) in a leaf-disc oxygen electrode (Hansatech, Kings Lynn) in saturating $^{14}CO_2$ at a PFD of 250 μmol m^{-2} s^{-1} of photosynthetically active radiation at 20°C for 30 min and subsequent fractionation was performed exactly as detailed by Lytovchenko et al. (2002). Fluorescence emission was measured in vivo using a pulse amplitude modulation fluorometer (Walz) on 6-week-old plants maintained at irradiances ranging from 100 to 800 μmol photons m^{-2} s^{-1} for 30 min prior to measurement of chlorophyll fluorescence yield and relative rate of electron transport calculated using the WinControl software package (Walz). Gas-exchange measurements were performed in a special custom-designed open system (Lytovchenko et al., 2002).

Measurement of Respiratory Parameters

Dark respiration was measured using the same gas exchange system as defined above. Estimations of the TCA cycle flux on the basis of $^{14}CO_2$ evolution were carried out following incubation of isolated leaf discs in 10 mM MES-KOH (pH 6.5) containing 2.32 KBq mL^{-1} of [1-^{14}C], [2-^{14}C], [3,4-^{14}C], or [6-^{14}C]Glc. $^{14}CO_2$ evolved was trapped in KOH and quantified by liquid scintillation counting. The results were interpreted following ap Rees and Beevers (1960).

Measurement of Redistribution of Isotope

The fate of ^{13}C-labeled pyruvate was traced following feeding of leaves excised from 6-week-old plants via the petiole placed in a solution containing 10 mM MES-KOH (pH 6.5) and 20 mM [U-^{13}C]pyruvate for 3 h. Fractional enrichment of metabolite pools was determined exactly as described previously (Roessner-Tunali et al., 2004; Tieman et al., 2006) and label redistribution was expressed as per Studart-Guimarães et al. (2007).

Statistical Analysis

The *t* tests were performed using the algorithm embedded into Microsoft Excel (Microsoft). The term significant is used in the text only when the change in question has been confirmed to be significant ($P < 0.05$).

Supplemental Data

The following materials are available in the online version of this article.

Supplemental Figure S1. Relative metabolite content of fully expanded leaves from 6-week-old plants of antisense mitochondrial citrate synthase lines.

Supplemental Figure S2. Differences in transcript levels between leaves of the well-characterized CS22 and wild type for genes associated with metabolism.

Supplemental Table S1. Enzyme activities in citrate synthase antisense transgenic lines.

ACKNOWLEDGMENTS

We gratefully acknowledge the excellent plant care of Helga Kulka, quantitative RT-PCR advice of Tomasz Czechowski, and the laboratory of Peter Dörmann for help with pigment analysis. We also thank Prof. Mark Stitt and Lothar Willmitzer for advice during the course of this work and Wioleta Wojtasik for technical support.

Received February 18, 2008; accepted March 16, 2008; published March 21, 2008.

LITERATURE CITED

Anoop VM, Basu U, McCammon MT, McAlister-Henn L, Taylor GJ (2003) Modulation of citrate metabolism alters aluminum tolerance in yeast and transgenic canola overexpressing mitochondrial citrate synthase. Plant Physiol **132:** 2205–2217

ap Rees T, Beevers H (1960) Pathways of glucose dissimilation in carrot slices. Plant Physiol **35:** 830–838

Bartoli CG, Gomez F, Gergoff G, Guiamet JJ, Puntarulo S (2005) Up-regulation of the mitochondrial alternative oxidase pathway enhances photosynthetic electron transport under drought conditions. J Exp Bot **56:** 1269–1276

Bassi R, Sandona D, Croce R (1997) Novel aspects of chlorophyll a/b-binding proteins. Physiol Plant **100:** 769–779

Baxter CJ, Liu JL, Fernie AR, Sweetlove LJ (2007) Determination of metabolic fluxes in a non-steady-state system. Phytochemistry **68:** 2313–2319

Bender-Machado L, Bauerlein M, Carrari F, Schauer N, Lytovchenko A, Gibon Y, Kelly AA, Loureiro M, Muller-Rober B, Willmitzer L, et al (2004) Expression of a yeast acetyl CoA hydrolase in the mitochondrion of tobacco plants inhibits growth and restricts photosynthesis. Plant Mol Biol **55:** 645–662

Bläsing OE, Gibon Y, Günther M, Höhne M, Morcuende R, Osuna D, Thimm O, Usadel B, Scheible WR, Stitt M (2005) Sugars and circadian regulation make major contributions to the global regulation of diurnal gene expression in *Arabidopsis*. Plant Cell **17:** 3257–3281

Campbell WH, Smarrelli J (1978) Purification and kinetics of higher plant NADH:nitrate reductase. Plant Physiol **61:** 611–616

Carrari F, Nunes-Nesi A, Gibon Y, Lytovchenko A, Ehlers Loureiro M, Fernie AR (2003) Reduced expression of aconitase results in an enhanced rate of photosynthesis and marked shifts in carbon partitioning in illuminated leaves of wild species tomato. Plant Physiol **133:** 1322–1335

Cornah JE, Smith SM (2002) Synthesis and function of glyoxylate cycled enzymes. *In* A Baker and IA Graham, eds, Plant Peroxisomes. Kluwer Academic Publishers, London, pp 57–101

Czechowski T, Bari RP, Stitt M, Scheible WR, Udvardi MK (2004) Real-time RT-sensitivity reveals novel root- and shoot-specific genes. Plant J **38:** 366–379

de la Fuente JM, Ramirez-Rodriguez V, Cabera-Ponce JL, Herrera-Estrella L (1997) Aluminium tolerance in transgenic plants by alteration of citrate synthase. Science **176:** 1566–1568

Delhaize E, Hebb DM, Ryan PR (2001) Expression of a *Pseudomonas aerugibos*a citrate synthase gene in tobacco is not associated with either enhanced citrate accumulation or efflux. Plant Physiol **125:** 2059–2067

Fahnenstich H, Saigo M, Niessen M, Zanor MI, Andreo CS, Fernie AR, Drincovich MF, Flügge UI, Maurino VG (2007) Alteration of organic acid metabolism in Arabidopsis overexpressing the maize C_4 NADP-

malic enzyme causes accelerated senescence during extended darkness. Plant Physiol **145:** 640–652

Farre EM, Tiessen A, Roessner U, Geigenberger P, Trethewey RN, Willmitzer L (2001) Analysis of the compartmentation of glycolytic intermediates, nucleotides, sugars, organic acids, and sugar alcohols in potato tubers using a nonaqueous fractionation method. Plant Physiol **127:** 685–700

Fernie AR, Carrari F, Sweetlove LJ (2004) Respiratory metabolism: glycolysis, the TCA cycle and mitochondrial electron transport chain. Curr Opin Plant Biol **7:** 254–261

Fernie AR, Roscher A, Ratcliffe RG, Kruger NJ (2001) Fructose 2,6-bisphosphate activates pyrophosphate: fructose 6 phosphate 1-phosphotransferase and increases triose phosphate to hexose phosphate cycling in heterotrophic cells. Planta **212:** 250–263

Friis JC, Holm C, Halling-Sorensen B (1998) Evaluation of elemental composition of algal biomass as toxical endpoint. Chemosphere **37:** 2665–2676

Fritz C, Palacios-Rojas N, Feil R, Stitt M (2006) Regulation of secondary metabolism by the carbon-nitrogen status in tobacco: nitrate inhibits large sectors of phenylpropanoid metabolism. Plant J **46:** 533–548

Galvez S, Bismuth E, Sarda C, Gadal P (1994) Purification and characterization of chloroplast NADP-isocitrate dehydrogenase from mixotrophic tobacco cells (comparison with the chloroplastic enzyme). Plant Physiol **105:** 593–600

Gaude N, Brehelin C, Tischendorf G, Kessler F, Dormann P (2007) Nitrogen deficiency in Arabidopsis affects galactolipid composition and gene expression and results in accumulation of fatty acid phytyl esters. Plant J **49:** 729–739

Gibon Y, Blaesing OE, Hannemann J, Carillo P, Hohne M, Hendriks JHM, Palacios N, Cross J, Selbig J, Stitt M (2004) A robot-based platform to measure multiple enzyme activities in *Arabidopsis* using a set of cycling assays: comparison of changes of enzyme activities and transcript levels during diurnal cycles and prolonged darkness. Plant Cell **16:** 3304–3325

Gibon Y, Usadel B, Blaesing OE, Kamlage B, Hoehne M, Trethewey R, Stitt M (2006) Integration of metabolite with transcript and enzyme activity profiling during diurnal cycles in Arabidopsis rosettes. Genome Biol **7:** R76

Higgins DG, Sharp PM (1988) CLUSTAL: a package for performing multiple sequence alignment on a microcomputer. Gene **73:** 237–244

Hodges M, Fleish V, Galves S, Bismuth E (2003) Higher plant NADP-dependent isocitrate dehydrogenases, ammonium assimilation and NADPH production. Plant Physiol Biochem **41:** 577–585

Hooks MA (2002) Molecular biology, enzymology, and physiology of β-oxidation. *In* A Baker and IA Graham, eds, Plant Peroxisomes. Kluwer Academic Publishers, London, pp 19–55

Igamberdiev AU, Romanowska E, Gardestrom P (2001) Photorespiratory flux and mitochondrial contribution to energy and redox balance of barley leaf protoplasts in the light and during light-dark transitions. J Plant Physiol **158:** 1325–1332

Ishizaki K, Larson TR, Schauer N, Fernie AR, Graham IA, Leaver CJ (2005) The critical role of *Arabidopsis* electron-transfer flavoprotein: ubiquinone oxidoreductase during dark-induced starvation. Plant Cell **17:** 2587–2600

Kochian LV, Hoekenga OA, Pineros MA (2004) How do crop plants tolerate acid soils? Mechanisms of aluminium tolerance and phosphorus efficiency. Annu Rev Plant Biol **55:** 459–493

Kopka J, Schauer N, Krueger S, Birkemeyer C, Usadel B, Bergmuller E, Dormann P, Weckwerth W, Gibon Y, Stitt M, et al (2005) GMD@CSB.DB: the Golm Metabolome Database. Bioinformatics **21:** 1635–1638

Landschütze V, Müller-Röber B, Willmitzer L (1995a) Mitochondrial citrate synthase from potato—dominant expression in mature leaves and young flower buds. Planta **196:** 756–764

Landschütze V, Willmitzer L, Müller-Röber B (1995b) Inhibition of flower formation by antisense repression of mitochondrial citrate synthase in transgenic potato plants leads to specific disintegration of the ovary tissues of flowers. EMBO J **14:** 660–666

Lea US, Slimestad R, Smedvig P, Lillo C (2007) Nitrogen deficiency enhances expression of specific MYB and bHLH transcription factors and accumulation of end products in the flavonoid pathway. Planta **225:** 1245–1253

Lemaitre T, Urbanczyk-Wochniak E, Flesch V, Bismuth E, Fernie AR, Hodges M (2007) NAD-dependent isocitrate dehydrogenase mutants of Arabidopsis suggest the enzyme is not limiting for nitrogen assimilation. Plant Physiol **144:** 1546–1558

Liu XJ, Prat S, Willmitzer L, Frommer WB (1999) Cis-regulatory elements directing tuber specific and sucrose inducible expression of a chimeric class I patatin promoter-GUS gene fusion. Mol Gen Genet **223:** 101–106

Lytovchenko A, Sweetlove LJ, Pauly M, Fernie AR (2002) The influence of cytosolic phosphoglucomutase on photosynthetic carbohydrate metabolism. Planta **215:** 1013–1021

Maldonado JM, Notton BA, Hewitt EJ (1978) Inhibitory effects of ferrocytochrome c on NADH-nitrate reductase activity of spinach (Spinacia oleracea L.). Plant Sci Lett **13:** 143–150

Manjunath S, Lee CHK, VanWinkle P, Bailey-Serres J (1998) Molecular and biochemical characterization of cytosolic phosphoglucomutase in maize—expression during development and in response to oxygen deprivation. Plant Physiol **117:** 997–1006

Mettler IJ, Beevers H (1980) Oxidation of NADH in glyoxysomes by a malate-aspartate shuttle. Plant Physiol **66:** 555–560

Nunes-Nesi A, Carrari F, Gibon Y, Sulpice R, Lytovchenko A, Fisahn J, Graham J, Ratcliffe RG, Sweetlove LJ, Fernie AR (2007) Deficiency of mitochondrial fumarase activity in tomato plants impairs photosynthesis via an effect on stomatal function. Plant J **50:** 1093–1106

Nunes-Nesi A, Carrari F, Lytovchenko A, Smith AMO, Ratcliffe RG, Sweetlove LJ, Fernie AR (2005) Enhanced photosynthetic performance and growth as a consequence of decreasing mitochondrial malate dehydrogenase activity in transgenic tomato plants. Plant Physiol **137:** 611–622

Orsel M, Chopin F, Leleu O, Smith SJ, Krapp A, Daniel-Vedel F, Miller AJ (2006) Characterisation of a two-component high-affinity nitrate uptake system in Arabidopsis. Physiology and protein-protein interaction. Plant Physiol **142:** 1304–1317

Picault N, Palmieri L, Pisano I, Hodges M, Palmieri F (2002) Identification of a novel transporter for dicarboxylates and tricarboxylates in plant mitochondria. Bacterial expression, reconstitution, functional characterization, and tissue distribution. J Biol Chem **277:** 24204–24211

Pracharoenwattana I, Cornah JE, Smith SM (2005) *Arabidopsis* peroxisomal citrate synthase is required for fatty acid respiration and seed germination. Plant Cell **17:** 2037–2048

Raghavendra AS, Padmasree K (2003) Beneficial interactions of mitochondrial metabolism with photosynthetic carbon assimilation. Trends Plant Sci **8:** 546–553

Raymond P, Spiteri A, Dieuaide M, Gerhardt B, Pradet A (1992) Peroxisomal beta-oxidation of fatty acids and citrate formation by a particulate fractionation from early germinating sunflower seeds. Plant Physiol Biochem **30:** 153–161

Roessner U, Luedemann A, Brust D, Fiehn O, Linke T, Willmitzer L, Fernie AR (2001) Metabolic profiling allows comprehensive phenotyping of genetically or environmentally modified plant systems. Plant Cell **13:** 11–29

Roessner-Tunali U, Hegemann B, Lytovchenko A, Carrari F, Bruedigam C, Granot D, Fernie AR (2003) Metabolic profiling of transgenic tomato plants overexpressing hexokinase reveals that the influence of hexose phosphorylation diminishes during fruit development. Plant Physiol **133:** 84–99

Roessner-Tunali U, Liu J, Leisse A, Balbo I, Perez-Melis A, Willmitzer L, Fernie AR (2004) Kinetics of labelling of organic and amino acids in potato tubers by gas chromatography-mass spectrometry following incubation in C-14 labelled isotopes. Plant J **39:** 668–679

Saitou N, Nei M (1987) The neighbor-joining method: a new method for reconstructing phylogenetic trees. Mol Biol Evol **4:** 406–425

Schauer N, Steinhauser D, Strelkov S, Schomburg D, Allison G, Moritz T, Lundgren K, Roessmer-Tunali U, Forbes MG, Willmitzer L, et al (2005) GC-MS libraries for the rapid identification of metabolites in complex biological samples. FEBS Lett **579:** 1332–1337

Scheibe R, Stitt M (1988) Comparison of NADP-malate dehydrogenase activation QA reduction and O2 evolution in spinach leaves. Plant Physiol Biochem **26:** 473–481

Scheible WR, Krapp A, Stitt M (2000) Reciprocal diurnal changes of phosphoenolpyruvate and NADP-isocitrate dehydrogenase expression regulate organic acid metabolism during nitrate assimilation in tobacco leaves. Plant Cell Environ **23:** 1155–1167

Studart-Guimarães C, Fait A, Nunes-Nesi A, Carrari F, Usadel B, Fernie AR (2007) Reduced expression of succinyl CoA ligase can be compensated for by an upregulation of the γ-amino-butyrate (GABA) shunt in illuminated tomato leaves. Plant Physiol **145:** 626–639

Sweetlove LJ, Fait A, Nunes-Nesi A, Williams T, Fernie AR (2007) The

mitochondrion: an integration point in cellular metabolism and signalling. Crit Rev Plant Sci **26:** 17–43

Sweetlove LJ, Lytovchenko A, Morgan M, Nunes-Nesi A, Taylor NL, Baxter CJ, Eickmeier I, Fernie AR (2006) Mitochondrial uncoupling protein is required for efficient photosynthesis. Proc Natl Acad Sci USA **103:** 19587–19592

Tamura K, Dudley J, Nei M, Kumar S (2007) MEGA4: Molecular Evolutionary Genetics Analysis (MEGA) software version 4.0. Mol Biol Evol **24:** 1596–1599

Tauberger E, Fernie AR, Emmermann M, Renz A, Kossmann J, Willmitzer L, Trethewey RN (2000) Antisense inhibition of plastidial phosphoglucomutase provides compelling evidence that potato tuber amyloplasts import carbon from the cytosol in the form of glucose 6-phosphate. Plant J **23:** 43–53

Tieman D, Taylor M, Schauer N, Fernie AR, Hanson AD, Klee HJ (2006) Tomato aromatic amino acid decarboxylases participate in synthesis of the flavor volatiles 2-phenylethanol and 2-phenylacetaldehyde. Proc Natl Acad Sci USA **103:** 8287–8292

Urbanczyk-Wochniak E, Usadel B, Thimm O, Nunes-Nesi A, Carrari F, Davy M, Blasing O, Kowalczyk M, Weicht D, Polinceusz A, et al (2006) Conversion of MapMan to allow the analysis of transcript data from Solanaceous species: effects of genetic and environmental alterations in energy metabolism in the leaf. Plant Mol Biol **60:** 773–792

Usadel B, Nagel A, Steinhauser D, Blasing OE, Redestig H, Sreenivasulu N, Krall L, Hannah MA, Poree F, Fernie AR (2006) An interactive ontology tool to generate, display, and annotate overview graphs for profiling experiments. BMC Bioinformatics **7:** 535

Usadel B, Nagel A, Thimm O, Redestig H, Blaesing OE, Palacios-Rojas N, Selbig J, Hannemann J, Piques MC, Steinhauser D, et al (2005) Extension of the visualization tool MapMan to allow statistical analysis of arrays, display of corresponding genes, and comparison with known responses. Plant Physiol **138:** 1195–1204

Van der Hoeven R, Ronning C, Giovannoni J, Martin G, Tanksley S (2003) Deductions about the number, organization and evolution of genes in the tomato genome based on analysis of a large expressed sequence tag collection and selective genomic sequencing. Plant Cell **14:** 1441–1456

Weeden NF, Gottlieb LD (1982) Dissociation, reassociation, and purification of plastid and cytosolic phosphoglucose isomerase isozymes. Plant Physiol **69:** 717–723

Yanagisawa S (2004) Dof domain proteins: plant-specific transcription factors associated with diverse phenomena unique to plants. Plant Cell Physiol **45:** 386–391

Yui R, Iketani S, Mikami T, Kubo T (2003) Antisense inhibition of mitochondrial pyruvate dehydrogenase E1 alpha subunit in anther tapetum causes male sterility. Plant J **34:** 57–66